



# Impairment of Global Lower Limb Muscle Coactivation During Walking in Cerebellar Ataxias

Lorenzo Fiori<sup>1,2,3</sup> · Alberto Ranavolo<sup>1</sup> · Tiwana Varrecchia<sup>1,4</sup> · Antonella Tatarelli<sup>1,5</sup> · Carmela Conte<sup>6</sup> · Francesco Draicchio<sup>1</sup> · Stefano Filippo Castiglia<sup>7</sup> · Gianluca Coppola<sup>7</sup> · Carlo Casali<sup>7</sup> · Francesco Pierelli<sup>7</sup> · Mariano Serrao<sup>7</sup>

Published online: 14 May 2020

© Springer Science+Business Media, LLC, part of Springer Nature 2020

## Abstract

The aim of this study was to investigate the time-varying multi-muscle coactivation function (TMCf) in the lower limbs during gait and its relationship with the biomechanical and clinical features of patients with cerebellar ataxia. A total of 23 patients with degenerative cerebellar ataxia (16 with spinocerebellar ataxia, 7 with adult-onset ataxia of unknown etiology) and 23 age-, sex-, and speed-matched controls were investigated. The disease severity was assessed using the Scale for the Assessment and Rating of Ataxia (SARA) in all patients. During walking, simultaneous acquisition of kinematic, kinetic, and electromyography data was performed using a motion analysis system. The coactivation was processed throughout the gait cycle using the TMCf, and the following parameters were measured: synthetic coactivation index, full width at half maximum, and center of activity. Spatiotemporal (walking speed, stance duration, swing duration, first and second double-support durations, step length, step width, stride length, Center of Mass displacement), kinetic (vertical component of GRFs), and energy consumption (total energy consumption and mechanical energy recovered) parameters were also measured. The coactivation variables were compared between patients and controls and were correlated with both clinical and gait variables. A significantly increased global TMCf was found in patients compared with controls. In addition, the patients showed a significant shift of the center of activity toward the initial contact and a significant reduction in energy recovery. All coactivation parameters were negatively correlated with gait speed, whereas the coactivation index and center of activity were positively correlated with both center-of-mass mediolateral displacement values and SARA scores. Our findings suggest that patients use global coactivation as a compensatory mechanism during the earliest and most challenging subphase (loading response) of the gait cycle to reduce the lateral body sway, thus improving gait stability at the expense of effective energy recovery. This information could be helpful in optimizing rehabilitative treatment aimed at improving lower limb muscle control during gait in patients with cerebella ataxia.

**Keywords** Ataxia · Gait analysis · Muscle coactivation

## Introduction

Gait ataxia is one of the most important features of degenerative cerebellar diseases. It is described as irregular

and wide-step walking with large variabilities in all global and segmental gait parameters [1–10], which lead to a loss of the physiological harmonic structure of the human gait [11]. Such gait abnormalities are present in various

✉ Lorenzo Fiori  
lor.fiori@libero.it

<sup>1</sup> Department of Occupational and Environmental Medicine, Epidemiology and Hygiene, INAIL, Monte Porzio Catone, Rome, Italy

<sup>2</sup> Department of Physiology and Pharmacology, Sapienza University of Rome, Rome, Italy

<sup>3</sup> PhD program in Behavioral Neuroscience, Sapienza University of Rome, Rome, Italy

<sup>4</sup> Department of Engineering, Roma TRE University, Rome, Italy

<sup>5</sup> Department of Human Neurosciences, Sapienza University of Rome, Rome, Italy

<sup>6</sup> Fondazione Don Gnocchi, Milan, Italy

<sup>7</sup> Department of Medico-Surgical Sciences and Biotechnologies, Sapienza University of Rome, Latina, Italy

locomotor tasks in daily life activities [7, 12–16] and inevitably worsen with the decline of gait function over time [11], thus predisposing patients to a high risk of falling in the early and intermediate stages (when they are still able to walk) [17–19] and causing them to lose their walking autonomy in the advanced stages of the disease [9].

In general, the ataxic gait reflects both the primary deficit, which is related to the lost ability of the cerebellum to process multi-sensory features and to provide an “error-correction mechanism” [6, 20, 21], and the compensatory mechanisms, which are used by patients to maintain dynamic stability during walking [7, 10, 22–24]. Beyond enlarging the base of support, another important compensatory strategy adopted by patients with cerebellar ataxia (CA) is to increase the coactivation of the antagonist muscles at a single-joint level, in an attempt to compensate for muscle hypotonia and irregular trajectories [8, 11, 16, 25, 26]. Furthermore, it has been demonstrated that patients with CA show widened muscle activation patterns with a significant temporal shift of the center of activity (CoA) [25]. These changes have also been observed in healthy individuals during unstable dynamic conditions (e.g., walking on a beam or on a slippery surface) [27], suggesting that the central nervous system (CNS) adopts a global compensatory strategy by involving the central pattern generators to deal with poor balance, namely by prolonging the duration of the basic patterns of muscle activity [27].

In a recent study [28], a new method for sample by sample analysis of the simultaneous coactivation of many muscles has been developed, proposing a time-varying multi-muscle coactivation function (TMCf). In healthy individuals, such global coactivation can be modulated to stabilize the limb during the most unstable (lower) or the most demanding (higher) gait speeds, allowing the adaptation to environmental demands and, at the same time, optimizing both energy consumption and energy recovery [29]. This method may enable understanding of the global strategy achieved by the CNS in modulating the activation/deactivation of many lower limb muscles during gait, irrespective of both the agonist-antagonist interaction at a single-joint level [16] and the modular architecture [30]. Our hypothesis herein is that patients with CA might be using a whole-limb compensatory strategy by coactivating many lower limb muscles to deal with the enlarged center-of-mass (CoM) oscillations, and that the coactivation might be correlated with the biomechanical and clinical features of patients with CA.

The aims of this study were as follows: (i) to investigate the TMCf in the lower limbs during gait in patients with CA; (ii) to compare the data of patients with CA with those of healthy subjects (HS); and (iii) to correlate the global coactivation parameters with the biomechanical (i.e., Center of Mass (CoM) displacement) and clinical features.

## Materials and Methods

### Subjects

Twenty-three patients (7 women, 16 men; age  $50.0 \pm 11.7$  years; weight  $70.2 \pm 12.4$  kg; height  $167.3 \pm 8.2$  cm) with degenerative CA were enrolled. Fourteen patients had a diagnosis of autosomal dominant ataxia (spinocerebellar ataxia [SCA]; eight with SCA1 and six with SCA2), whereas the other seven had sporadic adult-onset ataxia of unknown etiology (SAOA). The severity of the disease was rated using the Scale for the Assessment and Rating of Ataxia (SARA).

No patient was found to have visual impairment, whereas almost all patients had oculomotor abnormalities such as gaze nystagmus or square wave jerks during pursuit movements. All patients exhibited cerebellar atrophy on magnetic resonance imaging. Moreover, all patients were able to walk alone without any kind of aid on a level surface and to perform the required task. Because patients with SCA may show signs other than cerebellar features, we only included those who exhibited gait disturbances that were exclusively cerebellar in nature at the initial evaluation. The patients' characteristics are summarized in Table 1.

A total of 23 age-, sex-, and speed-matched HS were also enrolled as a control group (7 women, 16 men; age  $48.4 \pm 14.0$  years; weight  $73.2 \pm 14.5$  kg; height  $169.5 \pm 8.2$  cm).

All subjects provided informed consent before taking part in the study, which complied with the Helsinki Declaration and had local ethics committee approval.

### Procedure

All participants involved in the study were preliminary instructed about the correct experimental procedures and underwent practice tests to familiarize themselves with the experimental set up [31]. Each participant was asked to walk barefoot for approximately 8 m along the laboratory pathway while looking straight ahead. Patients with CA were asked to walk 10 times (10 trials) at a self-selected, comfortable speed. On the other hand, the HS were asked to walk 10 times at a self-selected speed and 10 times at a slow speed (slower than self-selected). Because we were interested in natural locomotion, only general, qualitative, and verbal instructions (no analog or digital metronomes were used) were provided. A 1-min break was provided between each walking trial to avoid the onset of muscle fatigue.

### Gait Analysis

For the acquisition of gait kinematics, a stereophotogrammetric motion analysis system with optoelectronic technology was used (SMART-D System; BTS, Italy, Milan). Eight infrared cameras (sampling rate 300 Hz) and 22

**Table 1** Patients' characteristics. SARA, Scale for the Assessment and Rating of Ataxia, SCA spinocerebellar ataxia, SAOA sporadic adult-onset ataxia

Patient	Gender	Age (years)	Body weight (kg)	Diagnosis	SARA (total)
CA1	M	69	107	SCA2	18
CA2	M	45	69	SCA2	15
CA3	F	65	67	SAOA	15
CA4	M	42	65	SCA1	7
CA5	M	37	69	SCA2	18
CA6	M	49	75	SAOA	9
CA7	M	32	51	SCA1	2
CA8	M	40	87	SCA2	22
CA9	F	55	67	SAOA	14
CA10	F	59	62	SAOA	12
CA11	F	72	58.5	SAOA	6
CA12	M	57	66	SAOA	9
CA13	M	45	80	SCA1	8
CA14	M	52	86.5	SCA1	8
CA15	F	56	55	SCA1	15
CA16	F	63	72	SAOA	10
CA17	F	48	67	SCA2	13
CA18	M	47	78	SAOA	15
CA19	M	49	74.5	SCA1	11
CA20	M	46	69	SAOA	12
CA21	M	33	51	SCA1	3
CA22	M	43	66	SCA1	8
CA23	M	46	71.5	SCA2	16

reflective markers positioned above the anatomical reference points were used, as previously reported [32]. In detail, the markers were positioned above the cutaneous projections of the spinous processes of the seventh cervical and sacral vertebra and bilaterally on the acromion, superior anterior iliac spine, large trochanter, lateral femoral condyle, fibula head, lateral malleoli, and metatarsal head. In addition to the markers directly applied to the skin, sticks or rods of variable length (from 7 to 10 cm) were used, positioned at one-third of the length of the body segment (femur and leg).

Ground reaction forces (GRFs) were acquired using two dynamometer platforms (Kistler 9286B; Kistler, Winterthur, Switzerland) that were longitudinally connected to each other but displaced by 0.2 m in the lateral direction (sampling rate 1200 Hz).

A wireless (Wi-Fi) 16-channel acquisition system (FreeEMG 1000; BTS SpA, Milan, Italy) was used to measure the superficial myoelectric activity. A preprocessing filtering and denoising procedure were performed. The lower and upper cutoff frequencies of the Hamming filter were 10 and 400 Hz, respectively, whereas the common mode rejection ratio was 100 dB (with a sampling frequency of 1 kHz). The probes were placed over the muscles of interest using Ag/AgCl pregelled electrodes (H124SG; Kendall ARBO, Donau, Germany) according to the recommendations of the *Atlas of*

*Muscle Innervation Zones* [33]. As the motor disturbances were symmetrical in our patients, we focused our analyses on the right-leg locomotor output. Therefore, the electrodes were placed over the following right-sided muscles: gluteus medius, rectus femoris, vastus lateralis, vastus medialis, tensor fascia latae, semitendinosus, biceps femoris, tibialis anterior, gastrocnemius medialis, gastrocnemius lateralis, soleus, and peroneus longus.

### Speed Matching Procedure

Given the expected slower gait in patients with CA than in controls, to avoid biases due to the speed dependency of kinematic and electromyographic (EMG) parameters, we matched the gait speed between the two groups. The walking speed matching procedure was performed as follows: (i) only strides in which the participants (patients and healthy controls) impacted the force platforms with heel were selected; (ii) for each ataxic patient, the average speed and the standard deviation of the selected steps were calculated; (iii) these mean values were used to select the steps in each age- and sex-matched control, at either self-selected or slow speed, such that the average value of the walking speed fell within the mean  $\pm$  SD of the corresponding ataxic patient (see Fig. 1a). Unpaired two-sample *t* test was used to verify that the mean

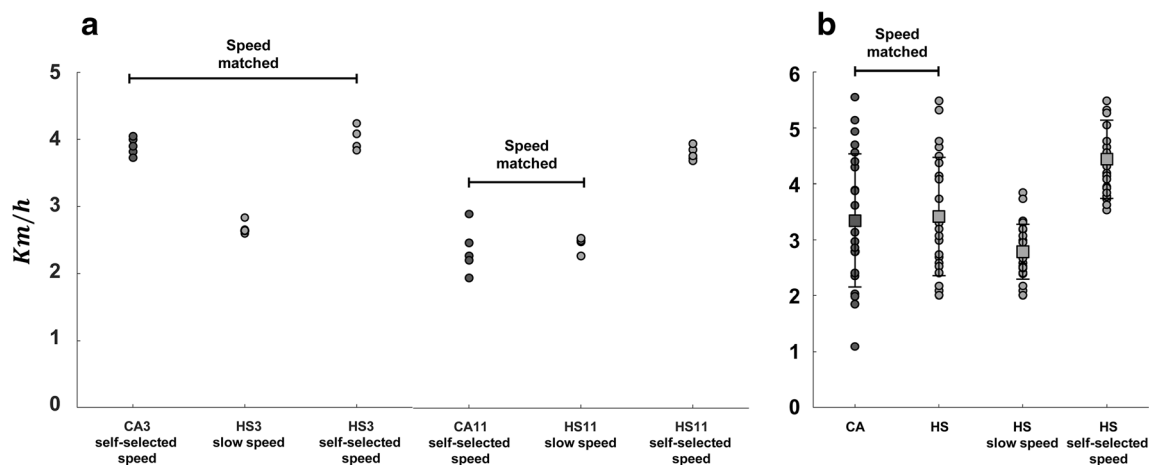


**Fig. 1** **a** Speed values for two representative patients with cerebellar ataxia (CA3 and CA11) and the speed values at self-selected and slow speeds for the age- and sex-matched healthy subjects (HS3 and HS11): CA3 was speed matched with self-selected speed of HS3 while CA11

was speed matched with slow speed of HS11. **b** Mean speed values ( $\pm$  SD) for CA and HS at speed matched, HS at slow speed, and mean speed values for each subject for CA and HS at speed matched, HS at slow speed, and HS at self-selected (circles)

speed values were not statistically different between groups (patients  $3.35 \pm 1.19$  km/h, controls  $3.42 \pm 1.04$  km/h,  $p = 0.83$ ,  $d = 0.06$ ; Fig. 1b).

## Data Analysis

All data were processed using the MATLAB R2018b calculation environment (version 9.5; MathWorks, Natick, MA, USA) and the Analyzer software (BTS). In order to obtain a complete data set of EMG, kinetic, and kinematics measurements during the “steady state” walking (avoiding the initial and terminal steps), we considered only the central strides in which the subject impacted the force platforms with heel. Since five was the minimum number of steps in which each participant struck the force platforms, we chose to analyze these five central strides for all participants.

## Surface EMG Parameters

The raw surface EMG (sEMG) signals were visually inspected to delete gait cycles with artifacts. Then the signals were filtered in the band of interest (20–450 Hz) with a Butterworth infinite impulse response digital band-pass filter of the fifth order to reduce movement artifacts (electrode-skin) and other components of high-frequency noise. Thereafter, to extract the muscle activity profile, an adaptive algorithm for the extraction of the sEMG envelope was applied [34].

For each subject, the elaborated sEMG signals of each muscle were amplitude-normalized with their peak values calculated over all steps considered and time-normalized to the duration of the cycle and reduced to 201 samples using a polynomial procedure [29]. The gait cycle was defined as the time between two

successive foot contacts of the same leg, and the heel-strike and toe-off events were determined [35].

From the processed sEMG signals, the simultaneous activation of the 12 lower limb muscles using the TMCf [28, 29, 35–38] was calculated. This method defines a time-dependent function, calculated as follows [29]:

$$TMCf(d(i), i) = \left(1 - \frac{1}{1 + e^{-a(d(i)-b)}}\right) \cdot \frac{(\sum_{m=1}^M EMG_m(i)/M)^2}{\max_{m=1 \dots M} [EMG_m(i)]}$$

where  $M$  is the number of muscles considered,  $EMG_m(i)$  is the sEMG sample value of the  $m$ th muscle at instant  $i$ ,  $a$ , and  $b$  are constants equal to 12 and 6 respectively [28], and  $d(i)$  is the mean of the differences between each pair among the 12  $EMG_m(i)$  samples at instant  $i$ :

$$d(i) = \left(\frac{\sum_{m=1}^{M-1} \sum_{n=m+1}^M |EMG_m(i) - EMG_n(i)|}{(M! / (2!(M-2)!))}\right)$$

where  $M! / (2!(M-2)!)$  is the total number of possible differences between each pair of  $EMG_m(i)$ .  $TMCf(d(i), i)$  is a function with values ranging between 0 and 100, which indicate absent and maximum coactivations, respectively.

The following parameters within the gait cycle were calculated: (i) the synthetic coactivation index (CI), which represents the average of the coactivation level (%), calculated as the mean value of the TMCf [28, 29]; (ii) the full width at half maximum of the TMCf ( $FWHM_{TMCf}$ ), which reflects the sum of the time durations within the gait cycle during which the TMCf curve is higher than its half maximum [29]; (iii) the CoA of the TMCf ( $CoA_{TMCf}$ ), which describes the position where the largest muscle coactivation occurs within the gait cycle [29].

Given the cyclic behavior of gait, it could be useful to transform and plot the data in polar coordinates (polar direction denotes the phase of the gait cycle, with angle  $\theta$  that varies from  $0^\circ$  to  $360^\circ$ ) that allow to express the continuity between the end of gait cycle (terminal swing subphase) and the onset of a new one (loading response subphase). For this, the  $CoA_{TMCf}$ , which contains spatiotemporal information, was calculated on the TMCf curves transformed in polar coordinates and it was also plotted in polar coordinates [25, 39].

The  $CoA_{TMCf}$  was calculated as the angle of the vector (first trigonometric moment) that points to the CoM of that circular distribution using the following formulas:

$$A = \sum_{i=1}^M (\cos\theta_i \times TMCf_i)$$

$$B = \sum_{i=1}^M (\sin\theta_i \times TMCf_i)$$

$$CoA = \tan^{-1}(A/B)$$

and (iv) the coefficient of multiple correlations (CMC), which measures the overall waveform similarity of a group of curves (the closer to 1 the CMC is, the more similar are the waveforms) [29, 40–42]. The CMC was calculated within subjects ( $CMC_{WS}$ ), between subjects ( $CMC_{BS}$ ), and between groups ( $CMC_{BG}$ ) using the mean curves of TMCf according to the following formula:

$$CMC = \sqrt{1 - \frac{\left(1/(T(N-1))\right) \sum_1^N i \sum_1^T t (y_{it} - \bar{y}_t)^2}{\left(1/(T(N-1))\right) \sum_1^N i \sum_1^T t (y_{it} - \bar{y})^2}}$$

where  $T = 201$  (number of points within the curve),  $N$  is the number of curves,  $y_{it}$  is the value at the  $t$ th point in the  $i$ th curve,  $\bar{y}_t$  is the average at point  $t$  over the 2 curves, and  $\bar{y}$  is the grand mean of all  $y_{it}$ .

**Kinetic Parameters**

The vertical component of GRFs (vertical force [VF]) was measured by the dynamometric platforms for each gait cycle and normalized both to the stance phase duration, using a polynomial interpolation procedure in 100 samples, and to each subject’s body weight [35].

To characterize the spatial and temporal profile of the VF curves, the indexes of the full width at half maximum ( $FWHM_{VF}$ ) and that of the CoA ( $CoA_{VF}$ ) [25, 29] were measured. In particular, the  $CoA_{VF}$  was evaluated using the same formula of  $CoA_{TMCf}$  where the polar direction denotes the phase of the stance cycle instead of gait cycle.

**Cross-Correlation Analysis**

Cross-correlation analysis [43] was used to evaluate the similarity in shape and timing between the VF and TMCf curves. The normalized cross-correlation function ( $R_{xy}(k)$ ) was calculated between the VF and TMCf mean curves of all subjects only for the stance phase, according to previous methods [29, 44]. In general, the  $R_{xy}(k)$  function shows similarity in shape and timing of events between two signals through the variation of amplitude (from 0 to 1) and the variation of distribution in time (from 0 to the total recorded duration in both positive and negative directions). We calculated the maximum value of  $R_{xy}(k)$  for both HS ( $R_{HS\_max}$ ) and patients with CA ( $R_{CA\_max}$ ) as a shape similarity index and the temporal shift between the 0 temporal point and the occurrence of  $R_{max}$ , ( $\tau_{HS}^*$ ), and ( $\tau_{CA}^*$ ) as the timing similarity index.

**Energetic Behavior**

The kinematic data were time-normalized to the duration of the cycle and reduced to 201 samples using a polynomial procedure.

To obtain information on the mechanical energy expenditure involving the whole skeletal muscle system during walking, we measured energy recovery and energy consumption in relation to the whole-body CoM [37, 45, 46].

The whole-body CoM was calculated using the “reconstructed pelvis method” [37, 47, 48] considering the kinematic data. In this method, the CoM coincides with the pelvic center, which is the geometric center of the triangle formed by the markers over the two anterior superior iliac spines and the sacrum.

For each subject’s CoM, the total mechanical energy ( $E_{tot}$ ) was calculated as sum of the kinetic ( $E_k$ ) and potential ( $E_p$ ) energies during the gait cycle.  $E_k$  was calculated as the sum of the kinematic energies on the  $x$  ( $E_{kx}$ ),  $y$  ( $E_{ky}$ ), and  $z$  ( $E_{kz}$ ) axes:

$$E_k = E_{kx} + E_{ky} + E_{kz} = \frac{1}{2} m (v_x^2 + v_y^2 + v_z^2)$$

where  $m$ ,  $v_x$ ,  $v_y$ , and  $v_z$  are the mass and velocity components of the CoM, respectively, whereas  $E_p$  was calculated as follows:

$$E_p = mgh$$

where  $h$  is the vertical ( $y$ ) CoM component and  $g$  is the gravitational acceleration.

The fraction of mechanical energy recovered during each walking step ( $R$ -step) [49] was calculated as follows:

$$R\text{-step} = \frac{W_p^+ + W_{kf}^+ - W_{tot}^+}{W_p^+ + W_{kf}^+} = \left(1 - \frac{W_{tot}^+}{W_p^+ + W_{kf}^+}\right)$$

where  $W_p^+$ ,  $W_{kf}^+$ , and  $W_{tot}^+$  represent the positive work (sum of the positive increments over one step) produced by the gravitational potential energy, kinetic energy of forward motion, and total mechanical energy, respectively. The total energy consumption (TEC) was calculated as follows [29, 45]:

$$TEC = \frac{W_{tot}^+}{0.21}$$

which has been normalized to the body weight and step length.

For each subject, the *R*-step and the normalized TEC values of all steps were averaged.

### Spatiotemporal Parameters

The following time-distance gait parameters were calculated for each subject: walking speed (km/h), stance duration (% gait cycle), swing duration (% gait cycle), first and second double-support durations (% gait cycle), step length (% limb length), step width (% limb length), stride length (% limb length), and displacement (m).

The coefficients of variation (CVs) of the step length, the step width, and stride length parameters were calculated as reported by Serrao et al. [14]:

$$CV = \frac{SD \cdot 100}{\text{mean}}$$

The CV is a measure of the variability of a data set, in which the closer to 0 the CV is, the less variable are the data.

### Statistical Analysis

All calculated parameters were averaged by considering five strides. A priori power analysis using the G\*Power computer program [50] indicated that a total sample of 21 participants would be needed to detect large effects ( $d = 0.8$ ) with 80% power using a *t* test for independent measures between means with  $\alpha = 0.05$ .

The Shapiro-Wilk test was used for the preliminary study of normal data distribution. The unpaired two-sample *t* test (ttest) or Mann-Whitney (MW) test was used to evaluate differences in kinematic, kinetic, spatiotemporal, energetic, and EMG data between patients with CA and HS.

We used the Watson-Williams test for circular data [51] which allows to compare mean angles with two or more samples and is equivalent, for angles, of an ANOVA/Kruskal-Wallis test. Specifically, we used this test to evaluate differences in CoA values, reported with polar representation, of both the TMCf and VF curves between patients with CA and HS.

A *p* value of  $< 0.05$  was considered statistically significant. Cohen's *d* values were evaluated to estimate the effect size,

considering small ( $< 0.5$ ), medium (from 0.5 to 0.8), and large ( $> 0.8$ ) effects.

The Pearson or Spearman test was used to investigate any correlations between global coactivation parameters and clinical and gait variables. Partial correlations were used to control for gait speed.

Statistical analysis was performed using MATLAB R2018b.

## Results

### Demographic Characteristics

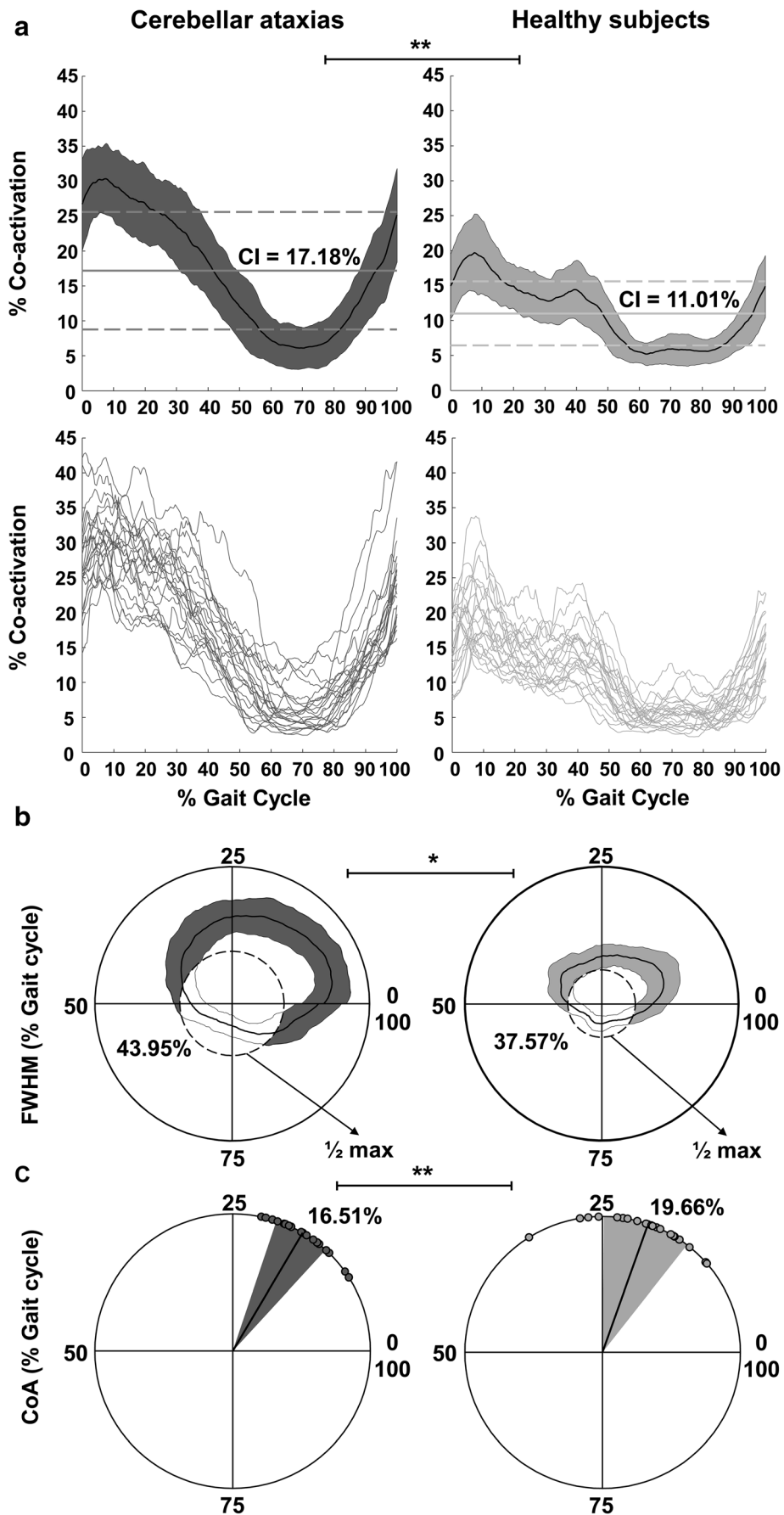
No significant differences were found between the CA and HS groups in terms of age ( $50.0 \pm 11.7$  years vs  $48.4 \pm 14.0$  years,  $p_{MW} = 0.58$ ), weight ( $70.2 \pm 12.4$  kg vs  $73.2 \pm 14.5$  kg,  $p_{MW} = 0.59$ ), and height ( $167.3 \pm 8.2$  cm vs  $169.5 \pm 8.2$  cm,  $p_{ttest} = 0.37$ ).

### sEMG Parameters

In Fig. 2 were reported the results of coactivation analysis for the 12 lower limb muscles during the gait cycle in both CA and HS. In detail, the upper graphs in Fig. 2 a show all TMCf curves of the 23 patients with CA (left graph) and of the 23 HS (right graph), whereas the lower graphs show the mean values of TMCf (average value in solid line and standard deviation [SD] in light color) with own CI (average value in solid line and SD in dotted line). Figure 2 b and c show the mean values of FWHM (presented with a polar graph and identified by the colored area between the curves) and of CoA (presented with a polar graph where the average values are the solid line and SD the circular sector in light color), respectively.

The global coactivation, in terms of both CI and FWHM of the TMCf, was significantly increased in patients with CA compared with HS (Fig. 2a, b). Furthermore, patients with CA shifted the global activation (i.e., CoATMCf) toward the initial contact (Fig. 2c). Specifically, patients with CA showed

**Fig. 2** Simultaneous coactivation of 12 lower limb muscles in patients with cerebellar ataxia (CA) and healthy subjects (HS). **a** Time-varying multi-muscle coactivation function (TMCf) curves: the upper graphs represent all TMCf curves of the 23 patients with CA and the 23 HS, whereas the lower graphs show the mean values of TMCf (average value in solid line and standard deviation [SD] in light color) with the coactivation index (CI) (average value in solid line and SD in dotted line). **b** Full width at half maximum (FWHM) of the TMCf: the TMCf (average and SD) is presented as a polar graph and the FWHM is the colored area subtending the curve. All quantities shown are expressed as a percentage of the gait cycle. **c** Center of activity (CoA) of the TMCf: each dot in the circumference represents an individual subject's mean CoA value, whereas the mean value and SD of the CoA of all subjects are represented by the solid line and the width of the circular sector (in light color), respectively



CI values of  $17.18 \pm 3.35\%$  vs values of  $11.01 \pm 1.81\%$  of the HS ( $p_{\text{ttest}} < 0.001$ ,  $d = 2.28$ ; see Fig. 2a) and  $\text{FWHM}_{\text{TMCf}}$  values of  $43.95 \pm 9.19\%$  vs values of  $37.57 \pm 8.70\%$  of the HS ( $p_{\text{ttest}} = 0.02$ ,  $d = 0.75$ ; see Fig. 2b), indicating a higher coactivation level. In addition, patients with CA showed lower values of CoA ( $16.51 \pm 3.31\%$ ) than HS ( $19.66 \pm 5.09\%$ ) ( $p = 0.001$ ; see Fig. 2c), indicating a shift of the global activation toward the initial contact (Fig. 2c).

Moreover, the CA patients showed higher TMCf waveform similarity both within and between subjects: the  $\text{CMC}_{\text{WS}}$  values were significantly higher than HS ( $\text{CMC}_{\text{WS}}$   $0.89 \pm 0.04$  vs.  $0.85 \pm 0.06$ ,  $p_{\text{MW}} = 0.005$ ,  $d = 0.85$ ) and the  $\text{CMC}_{\text{BS}}$  values higher than HS ( $\text{CMC}_{\text{BS}}$   $0.84$  vs.  $0.80$ ). Lastly, a lower value of TMCf waveform similarity between groups ( $\text{CMC}_{\text{BG}} = 0.70$ ) was found.

### Kinetic Parameters

The VFs of both patients with CA and the HS are shown in Fig. 3 a as averaged curves and standard deviations, while Fig. 3 b and c show the mean values of FWHM (identified by the colored area between the curves) and of CoA (average values are the solid line and SD the circular sector in light color), respectively. No significant difference was observed for  $\text{FWHM}_{\text{VF}}$  ( $83.47 \pm 7.19\%$  vs  $83.37 \pm 4.45\%$ ;  $p_{\text{ttest}} = 0.95$  see Fig. 3b) whereas a significantly lower value of  $\text{CoA}_{\text{VF}}$  was found in patients with CA than in HS ( $49.73 \pm 4.01\%$  vs  $52.52 \pm 1.31\%$ ,  $p = 0.001$ ; see Fig. 3c),

### Cross-Correlation Analysis

Figure 4 shows the results of the cross-correlation between the TMCf and VF averaged curve values within the HS (Fig. 4a) and CA groups (Fig. 4b), with the maximum point ( $R_{\text{max}}$ ) and the time of its occurrence ( $\tau^*$ ) obtained through a comparison of the curves. The figure demonstrates that both the groups showed a high degree of similarity:  $R_{\text{HS\_max}}$  was 0.96 and  $R_{\text{CA\_max}}$  was 0.94. Furthermore, the same values of  $\tau^*$  were observed for the two groups:  $\tau^*_{\text{HS}}$  and  $\tau^*_{\text{CA}}$  were 9% (Fig. 4b).

### Energetic Behavior

Significantly lower  $R$ -step values were found in the CA group than in the HS group ( $45.14 \pm 9.52\%$  vs  $4.66 \pm 6.50\%$ ,  $p_{\text{ttest}} < 0.001$ ;  $d = 1.17$ ). No significant TEC values were found in patients with CA compared with HS ( $0.54 \pm 0.11$  kcal/km · kg vs  $0.53 \pm 0.09$  kcal/km · kg;  $p_{\text{ttest}} = 0.51$ ;  $d = 0.11$ ).

### Spatiotemporal Parameters

Patients with CA showed significantly lower values than HS of stride length ( $1.10 \pm 0.34\%$  limb length vs  $1.28 \pm 0.18\%$  limb length,  $p_{\text{ttest}} = 0.03$ ,  $d = 0.66$ ) and significantly higher

values than HS of in step width ( $0.33 \pm 0.06\%$  limb length vs  $0.25 \pm 0.03\%$  limb length,  $p_{\text{ttest}} < 0.0001$ ,  $d = 1.65$ ), CV's step length ( $6.82 \pm 5.04$  vs  $3.35 \pm 1.69$ ,  $p_{\text{MW}} < 0.001$ ,  $d = 0.92$ ), CV's step width ( $9.89 \pm 6.02$  vs  $6.74 \pm 1.96$ ,  $p_{\text{ttest}} = 0.02$ ,  $d = 0.71$ ), CV's stride length ( $6.88 \pm 5.22$  vs  $3.89 \pm 2.57$ ,  $p_{\text{MW}} = 0.02$ ,  $d = 0.73$ ), and CoM mediolateral displacement ( $0.08 \pm 0.03$  m vs  $0.07 \pm 0.03$  m,  $p_{\text{MW}} = 0.04$ ,  $d = 0.78$ ). Whereas no significant differences were found between the CA and HS groups in stance duration ( $66.68 \pm 3.73\%$  gait cycle vs  $65.58 \pm 2.93\%$  gait cycle,  $p_{\text{ttest}} = 0.27$ ,  $d = 0.33$ ), swing duration ( $33.32 \pm 3.73\%$  gait cycle vs  $34.42 \pm 2.93\%$  gait cycle,  $p_{\text{ttest}} = 0.27$ ,  $d = 0.33$ ), 1st double support ( $16.42 \pm 3.38\%$  gait cycle vs  $15.68 \pm 2.82\%$  gait cycle,  $p_{\text{ttest}} = 0.43$ ,  $d = 0.24$ ), 2nd double support ( $16.91 \pm 4.64\%$  gait cycle vs  $15.42 \pm 2.88\%$  gait cycle,  $p_{\text{MW}} = 0.27$ ,  $d = 0.38$ ), step length ( $0.66 \pm 0.12\%$  limb length vs  $0.70 \pm 0.08\%$  limb length,  $p_{\text{ttest}} = 0.28$ ,  $d = 0.32$ ).

### Correlation

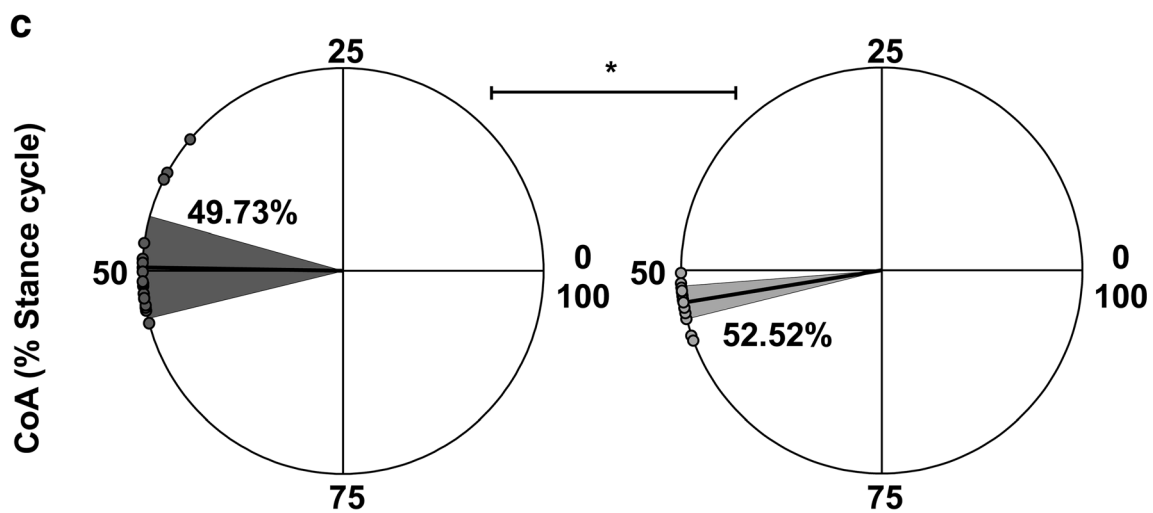
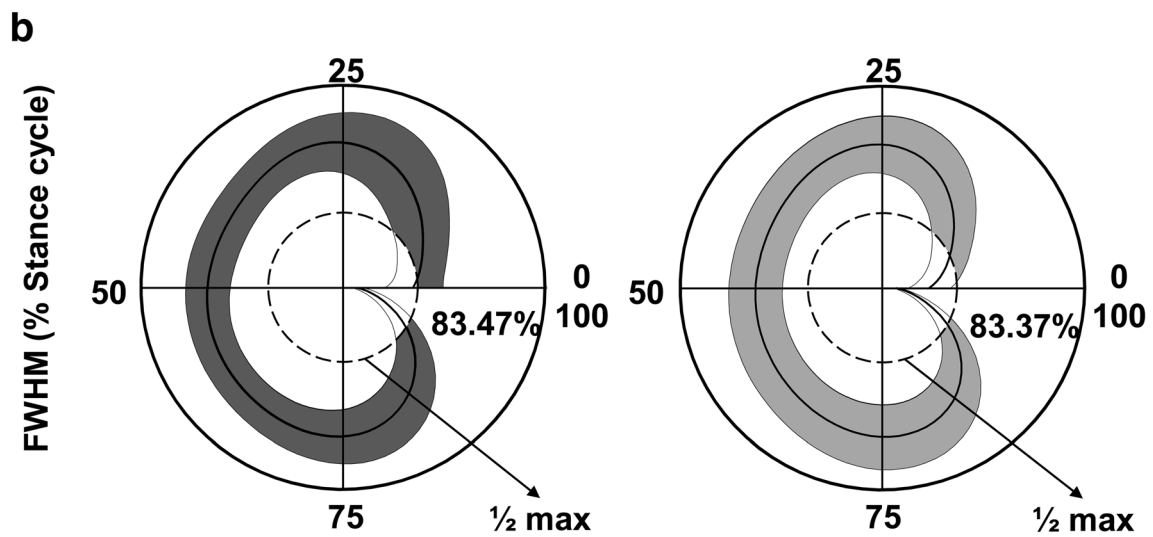
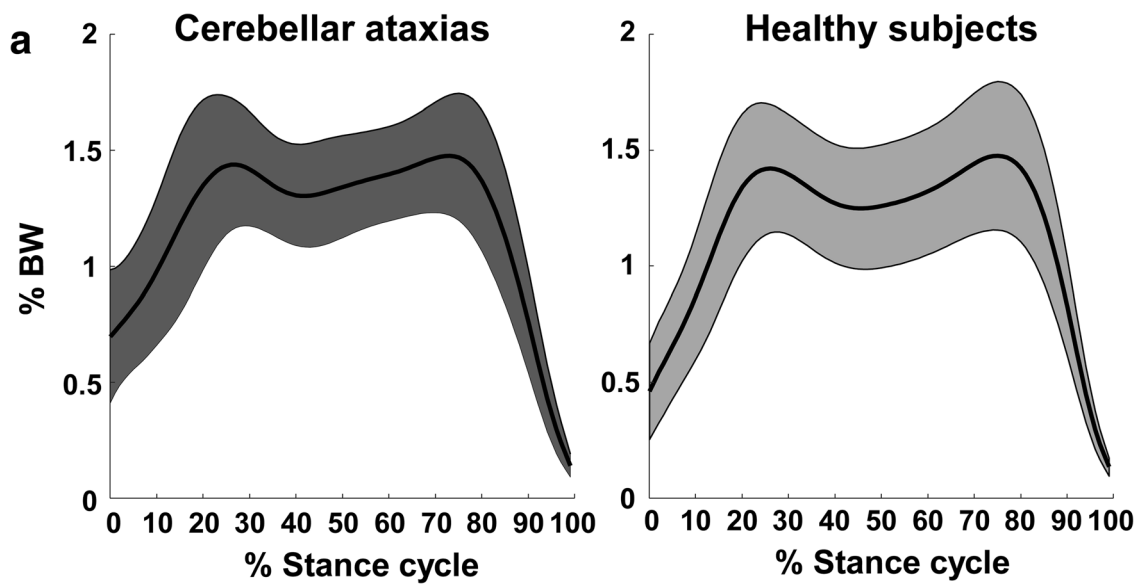
Figure 5 shows the negative moderate correlation between gait speed and CI ( $r = -0.65$ ,  $p = 0.002$ ),  $\text{CoA}_{\text{TMCf}}$  ( $r = -0.60$ ,  $p = 0.005$ ) and  $\text{FWHM}_{\text{TMCf}}$  ( $r = -0.59$ ,  $p = 0.005$ ). Furthermore, Fig. 5 shows a significant positive partial correlation between CI and both CoM mediolateral displacement values ( $r = 0.54$ ,  $p = 0.01$ ) and SARA scores ( $r = 0.45$ ,  $p = 0.04$ ) and between  $\text{CoA}_{\text{TMCf}}$  and both CoM mediolateral displacement values ( $r = 0.55$ ,  $p = 0.01$ ) and SARA scores ( $r = 0.46$ ,  $p = 0.03$ ).

### Discussion

The main results of this study can be summarized as follows: (i) global coactivation was significantly increased in patients with CA compared with HS, in terms of both CI and  $\text{FWHM}_{\text{TMCf}}$ ; (ii) patients with CA shifted the global activation  $\text{CoA}_{\text{TMCf}}$  toward the initial contact; and (iii) the global coactivation parameters were negatively correlated with gait speed and positively correlated with both CoM lateral displacement and SARA scores, whereas there was a lack of correlation with energetic parameters and gait variability.

In our study, patients with CA showed a significantly marked (Cohen  $d > 0.8$ ) increase in global coactivation, in





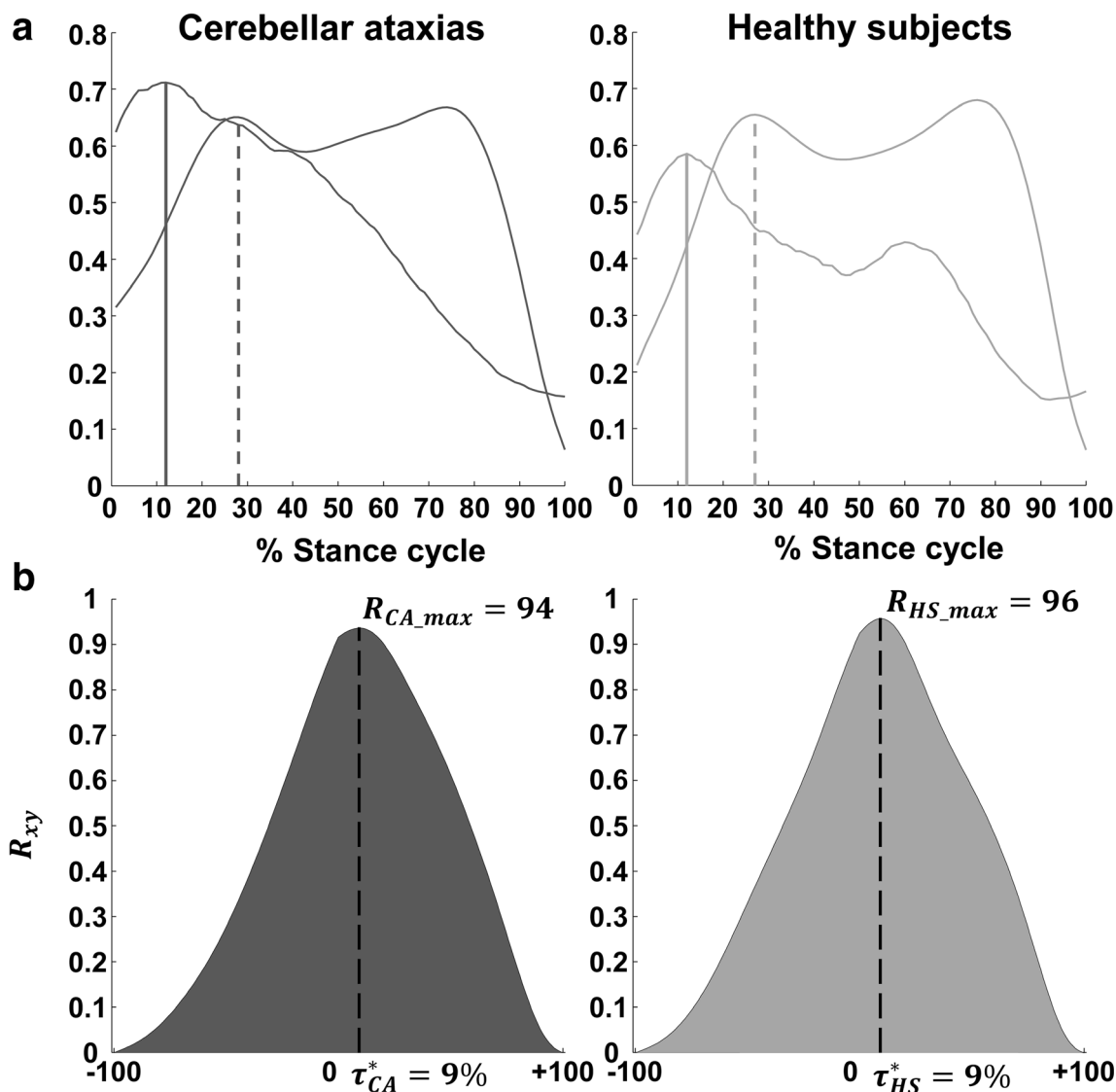


**Fig. 4** Cross-correlation. **a** Mean curves of time-varying multi-muscle coactivation function (TMCf) (continuous line) and vertical force (VF) (dashed line), normalized to the maximum value among all subjects, presented in the range of 0–1. **b** Cross-correlation curves between the

TMCf and the VF curves and their relative maximum value ( $R_{max}$ ). The dashed lines represent the temporal shift ( $\tau^*$ ) of the cross-correlation. All quantities shown are expressed as a percentage of the stance phase of the gait cycle

terms of both CI and  $FWHM_{TMCf}$ , compared with HS. Furthermore, they also showed a shift of the  $CoA_{TMCf}$  toward the earlier subphase of the gait cycle compared with HS (i.e., initial contact; in the clockwise direction, as illustrated in Fig. 2c). These findings seem to suggest that patients with CA increase the coactivation as a compensatory mechanism mainly during the loading response subphase, which represents the most challenging biomechanical condition, when the body weight is shifted from one limb to another and a response to the perturbation induced by the GRF is needed [32, 52]. In this regard, the correlation between  $CoA_{TMCf}$  and both the CoM lateral displacement and SARA score strongly suggests that increased coactivation is a global compensatory mechanism to cope with the enlarged lateral body sway resulting from the lack of interjoint coordination and hypotonia, which, in turn,

are caused by cerebellar degeneration. However, the lack of correlation with the R-step in CA, which is present in HS [29], indicates that such a compensatory mechanism compromises the ability of patients to recover energy during walking.

Interestingly, despite the global coactivation and GRF CoA shifts (Figs. 2 and 3) in the CA group compared with the HS group, no significant differences were found in the cross-correlation analysis between the global coactivation and GRF curves in patients with CA (Fig. 4). Notwithstanding the cerebellar degeneration, patients with CA maintained the same spatiotemporal relationship between muscle coactivation and foot-ground interaction torques as the HS [29], suggesting that the cerebellum is not involved in such a motor control mechanism. This concept is further reinforced by the observation that the coactivation curve similarity, as

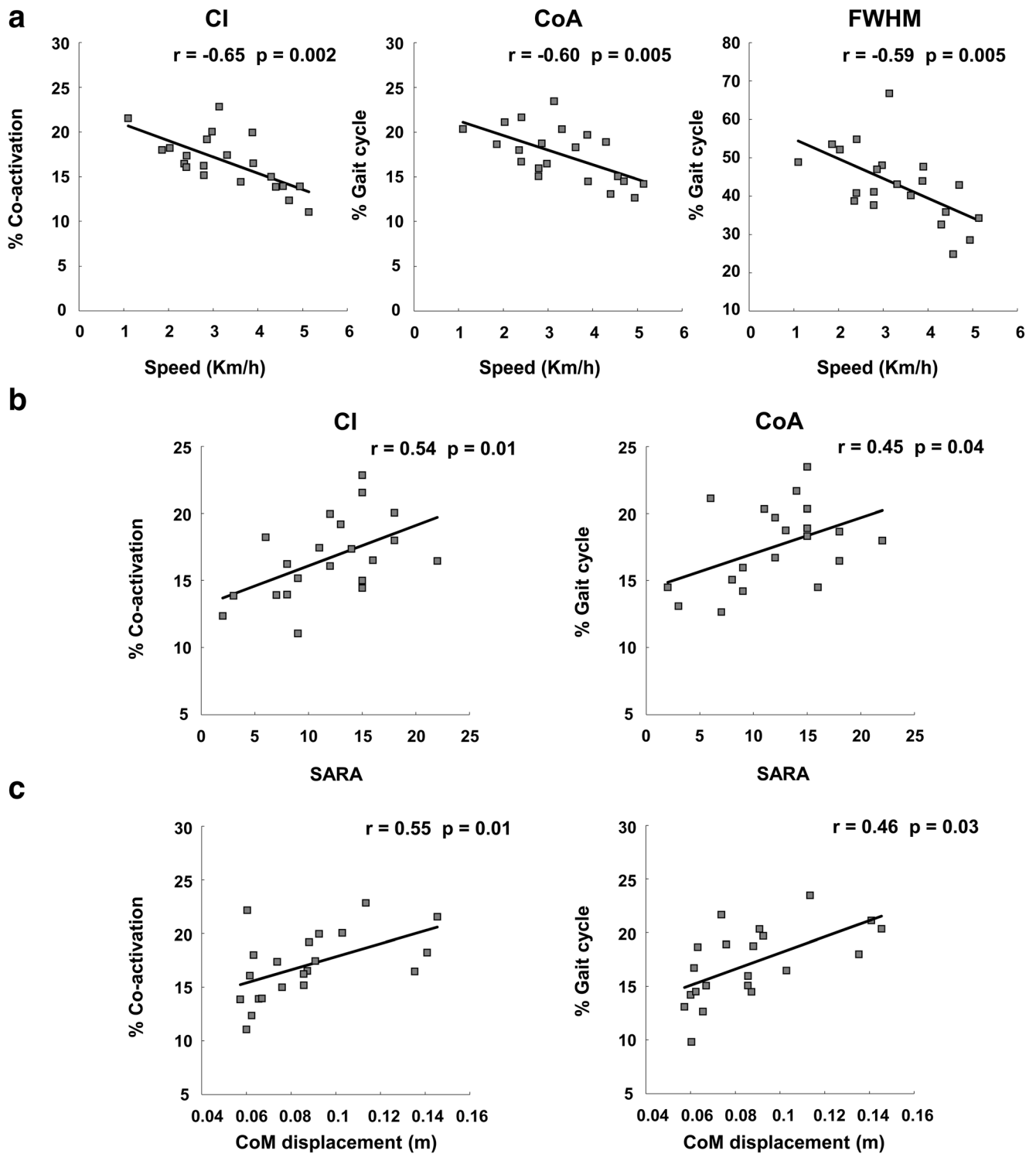


**Fig. 5** Correlations among the time-varying multi-muscle coactivation function (TMCf) parameters, gait parameters, and clinical scores. Only parameters that significantly differed between patients with cerebellar ataxia and healthy subjects are plotted in this figure. Each point on the graphs represents the value for the individual patient, and linear regression lines (solid line) with corresponding  $r$  and  $p$  values are reported. **a**

Relationships of the coactivation index (CI), center of activity (CoA), and full width at half maximum (FWHM) to the mean gait speed. **b** CI and CoA with the Scale for the Assessment and Rating of Ataxia (SARA) score. **c** CI and CoA with the center-of-mass mediolateral displacement

evaluated using the CMCs, was higher in patients with CA than in HS. In addition, as the global coactivation curve peak

preceded the GRF peak (Fig. 4), a plausible interpretation of the overall results is that patients with CA have increased level

of global activation to both control and respond to the GRF, which involves CNS structures other than the cerebellum, in an attempt to minimize the CoM lateral displacements through a feedforward mechanism [53, 54].

In our study, although patients with CA typically showed increased gait variability, no significant correlations were found with the global coactivation parameters. These findings suggest that global coactivation is uniquely exerted to minimize the CoM displacement rather than to stabilize the limb motion and reduce the gait variability, as reported for single-joint muscle coactivation [16]. Thereby, both global and single-joint coactivations seem to deal with different aspects of dynamic balance control.

A potential technical limitation of this study is that the TMCf profile is strictly dependent on the normalization technique adopted. As we normalized the lower limb muscle sEMG signals to the peak values across all trials, the normalization to the maximal voluntary contraction was not considered. However, our choice was made because the maximal voluntary contraction can be lengthy and hardly executable in patients with motor impairment, thus making the normalization poorly reliable [55].

In conclusion, the strength of this study lies in the use of a novel method for investigating coactivation in patients with gait ataxia disorder. Our results provided a time-varying characterization, within the gait cycle, of the simultaneous activation of 12 lower limb muscles at a multi-joint level, without requiring an a priori sorting of the agonist-antagonist muscles. In detail, we observed increased global coactivation, which likely reflects a compensatory mechanism adopted by patients to stiffen the whole limb and to cope with the enlarged lateral body sway. Such knowledge on how patients can increase or reduce the coactivation of lower limb muscles within the gait cycle may improve the ability of physicians to optimize rehabilitation strategies and may help technicians in designing new types of orthoses.

## Compliance with Ethical Standards

**Conflict of Interest** The authors declare that they have no conflict of interest.

## References

1. Earhart GM, Bastian AJ. Selection and coordination of human locomotor forms following cerebellar damage. *J Neurophysiol* [Internet]. American Physiological SocietyBethesda, MD; 2001 [cited 2019 Jul 11];85:759–69. Available from: <https://doi.org/10.1152/jn.2001.85.2.759>
2. Stolze H, Klebe S, Petersen G, Raethjen J, Wenzelburger R, Witt K, et al. Typical features of cerebellar ataxic gait. *J Neurol Neurosurg Psychiatry* [Internet]. BMJ Publishing Group Ltd; 2002 [cited 2019 Jul 11];73:310–2. Available from: <http://www.ncbi.nlm.nih.gov/pubmed/12185166>
3. Morton SM, Bastian AJ. Relative contributions of balance and voluntary leg-coordination deficits to cerebellar gait ataxia. *J Neurophysiol* [Internet]. American Physiological SocietyBethesda, MD; 2003 [cited 2019 Jul 11];89:1844–56. Available from: <https://doi.org/10.1152/jn.00787.2002>
4. Ilg W, Golla H, Thier P, Giese MA. Specific influences of cerebellar dysfunctions on gait. *Brain* [Internet]. Narnia; 2007 [cited 2019 Jul 11];130:786–98. Available from: <https://doi.org/10.1093/brain/awl376>
5. Ilg W, Branscheidt M, Butala A, Celnik P, de Paola L, Horak FB, et al. Consensus Paper: Neurophysiological assessments of ataxias in daily practice. *The Cerebellum* [Internet]. Springer US; 2018 [cited 2019 Jul 11];17:628–53. Available from: <https://doi.org/10.1007/s12311-018-0937-2>
6. Ilg W, Timmann D. Gait ataxia-specific cerebellar influences and their rehabilitation. *Mov Disord* [Internet]. John Wiley & Sons, Ltd; 2013 [cited 2019 Jul 11];28:1566–75. Available from: <https://doi.org/10.1002/mds.25558>
7. Serrao M, Pierelli F, Ranavolo A, Draicchio F, Conte C, Don R, et al. Gait pattern in inherited cerebellar ataxias. *The Cerebellum* [Internet]. Springer-Verlag; 2012 [cited 2019 Jul 11];11:194–211. Available from: <https://doi.org/10.1007/s12311-011-0296-8>
8. Serrao M. Rehabilitation of ataxias. Springer, Cham; 2018 [cited 2019 Jul 11]. p. 195–200. Available from: [https://doi.org/10.1007/978-3-319-72736-3\\_13](https://doi.org/10.1007/978-3-319-72736-3_13)
9. Serrao M, Conte C. Detecting and measuring ataxia in gait. *Handb Hum Motion* [Internet]. Cham: Springer International Publishing; 2018 [cited 2019 Jul 11]. p. 937–54. Available from: [https://doi.org/10.1007/978-3-319-14418-4\\_46](https://doi.org/10.1007/978-3-319-14418-4_46)
10. Serrao M, Ranavolo A, Casali C. Neurophysiology of gait. *Handb Clin Neurol* [Internet]. Elsevier; 2018 [cited 2019 Jul 11];154:299–303. Available from: <https://www.sciencedirect.com/science/article/pii/B9780444639561000187>
11. Serrao M, Chini G, Iosa M, Casali C, Morone G, Conte C, et al. Harmony as a convergence attractor that minimizes the energy expenditure and variability in physiological gait and the loss of harmony in cerebellar ataxia. *Clin Biomech (Bristol, Avon)* [Internet]. Elsevier; 2017 [cited 2019 Jul 11];48:15–23. Available from: <http://www.ncbi.nlm.nih.gov/pubmed/28704694>
12. Serrao M, Conte C, Casali C, Ranavolo A, Mari S, Di Fabio R, et al. Sudden stopping in patients with cerebellar ataxia. *The Cerebellum* [Internet]. Springer US; 2013 [cited 2019 Jul 11];12:607–16. Available from: <https://doi.org/10.1007/s12311-013-0467-x>
13. Serrao M, Mari S, Conte C, Ranavolo A, Casali C, Draicchio F, et al. Strategies Adopted by cerebellar ataxia patients to perform uturns. *The Cerebellum* [Internet]. Springer US; 2013 [cited 2019 Jul 11];12:460–8. Available from: <https://doi.org/10.1007/s12311-012-0441-z>
14. Conte C, Serrao M, Casali C, Ranavolo A, Silvia M, Draicchio F, et al. Planned gait termination in cerebellar ataxias. *The Cerebellum* [Internet]. Springer-Verlag; 2012 [cited 2019 Jul 11];11:896–904. Available from: <https://doi.org/10.1007/s12311-011-0348-0>
15. Conte C, Pierelli F, Casali C, Ranavolo A, Draicchio F, Martino G, et al. Upper body kinematics in patients with cerebellar ataxia. *The Cerebellum* [Internet]. Springer US; 2014 [cited 2019 Jul 11];13:689–97. Available from: <https://doi.org/10.1007/s12311-014-0586-z>
16. Mari S, Serrao M, Casali C, Conte C, Martino G, Ranavolo A, et al. Lower limb antagonist muscle co-activation and its relationship with gait parameters in cerebellar ataxia. *The Cerebellum* [Internet]. Springer US; 2014 [cited 2019 Jul 11];13:226–36. Available from: <https://doi.org/10.1007/s12311-013-0533-4>
17. van de Warrenburg BPC, Steijns JAG, Munneke M, Kremer BPH, Bloem BR. Falls in degenerative cerebellar ataxias. *Mov Disord* [Internet]. John Wiley & Sons, Ltd; 2005 [cited 2019 Jul 11];20:497–500. Available from: <https://doi.org/10.1002/mds.20375>

18. Schniepp R, Wuehr M, Schlick C, Huth S, Pradhan C, Dieterich M, et al. Increased gait variability is associated with the history of falls in patients with cerebellar ataxia. *J Neurol* [Internet]. Springer Berlin Heidelberg; 2014 [cited 2019 Jul 11];261:213–23. Available from: <https://doi.org/10.1007/s00415-013-7189-3>
19. Schniepp R, Schlick C, Pradhan C, Dieterich M, Brandt T, Jahn K, et al. The interrelationship between disease severity, dynamic stability, and falls in cerebellar ataxia. *J Neurol* [Internet]. Springer Berlin Heidelberg; 2016 [cited 2019 Jul 11];263:1409–17. Available from: <https://doi.org/10.1007/s00415-016-8142-z>
20. Morton SM, Bastian AJ. Cerebellar control of balance and locomotion. *Neurosci* [Internet]. Sage Publications/Sage CA: Thousand Oaks, CA; 2004 [cited 2019 Jul 11];10:247–59. Available from: <https://doi.org/10.1177/1073858404263517>
21. Konczak J, Timmann D. The effect of damage to the cerebellum on sensorimotor and cognitive function in children and adolescents. *Neurosci Biobehav Rev* [Internet]. Pergamon; 2007 [cited 2019 Jul 11];31:1101–13. Available from: <https://www.sciencedirect.com/science/article/pii/S0149763407000504>
22. Bodranghien F, Bastian A, Casali C, Hallett M, Louis ED, Manto M, et al. Consensus paper: revisiting the symptoms and signs of cerebellar syndrome. *The Cerebellum* [Internet]. Springer US; 2016 [cited 2019 Jul 11];15:369–91. Available from: <https://doi.org/10.1007/s12311-015-0687-3>
23. Vasco G, Gazzellini S, Petrarca M, Lispi ML, Pisano A, Zazza M, et al. Functional and gait assessment in children and adolescents affected by Friedreich’s ataxia: A One-Year Longitudinal Study. Palau F, editor. *PLoS One* [Internet]. Public Library of Science; 2016 [cited 2019 Jul 11];11:e0162463. Available from: <https://doi.org/10.1371/journal.pone.0162463>
24. Caliandro P, Iacovelli C, Conte C, Symbolotti C, Rossini PM, Padua L, et al. Trunk-lower limb coordination pattern during gait in patients with ataxia. *Gait Posture* [Internet]. Elsevier; 2017 [cited 2019 Jul 11];57:252–7. Available from: <https://www.sciencedirect.com/science/article/abs/pii/S0966636217304903?via%3Dihub>
25. Martino G, Ivanenko YP, Serrao M, Ranavolo A, d’Avella A, Draicchio F, et al. Locomotor patterns in cerebellar ataxia. *J Neurophysiol* [Internet]. American Physiological Society Bethesda, MD; 2014 [cited 2019 Jul 11];112:2810–21. Available from: <http://www.physiology.org/doi/10.1152/jn.00275.2014>
26. Conte C, Serrao M, Cuius L, Ranavolo A, Conforto S, Pierelli F, et al. Effect of restraining the base of support on the other biomechanical features in patients with cerebellar ataxia. *The Cerebellum* [Internet]. Springer US; 2018 [cited 2019 Jul 11];17:264–75. Available from: <https://doi.org/10.1007/s12311-017-0897-y>
27. Martino G, Ivanenko YP, d’Avella A, Serrao M, Ranavolo A, Draicchio F, et al. Neuromuscular adjustments of gait associated with unstable conditions. *J Neurophysiol* [Internet]. American Physiological Society Bethesda, MD; 2015 [cited 2019 Jul 11];114:2867–82. Available from: <http://www.physiology.org/doi/10.1152/jn.00029.2015>
28. Ranavolo A, Mari S, Conte C, Serrao M, Silvetti A, Iavicoli S, et al. A new muscle co-activation index for biomechanical load evaluation in work activities. *Ergonomics* [Internet]. Taylor & Francis; 2015 [cited 2019 Jul 11];58:966–79. Available from: <https://doi.org/10.1080/00140139.2014.991764>
29. Varrecchia T, Rinaldi M, Serrao M, Draicchio F, Conte C, Conforto S, et al. Global lower limb muscle coactivation during walking at different speeds: Relationship between spatio-temporal, kinematic, kinetic, and energetic parameters. *J Electromyogr Kinesiol* [Internet]. Elsevier; 2018 [cited 2019 Jul 11];43:148–57. Available from: <https://www.sciencedirect.com/science/article/pii/S1050641118301949?via%3Dihub>
30. Ivanenko YP, Cappellini G, Solopova IA, Grishin AA, MacLellan MJ, Poppele RE, et al. Plasticity and modular control of locomotor patterns in neurological disorders with motor deficits. *Front Comput Neurosci* [Internet]. Frontiers; 2013 [cited 2019 Jul 11];7:123. Available from: <https://doi.org/10.3389/fncom.2013.00123/abstract>
31. Hamacher D, Hamacher D, Krowicki M, Schega L. Between-day test–retest reliability of gait variability in older individuals improves with a familiarization trial. *Aging Clin Exp Res* [Internet]. Springer International Publishing; 2017 [cited 2019 Jul 22];29:327–9. Available from: <https://doi.org/10.1007/s40520-016-0536-3>
32. Davis RB, Öunpuu S, Tyburski D, Gage JR. A gait analysis data collection and reduction technique. *Hum Mov Sci* [Internet]. North-Holland; 1991 [cited 2019 Jul 11];10:575–87. Available from: <https://www.sciencedirect.com/science/article/abs/pii/016794579190046Z>
33. Barbero M, Merletti R, Rainoldi A. Atlas of muscle innervation zones : understanding surface electromyography and its applications [Internet]. Springer; 2012 [cited 2019 Jul 11]. Available from: [https://books.google.it/books?hl = it&lr = &id = rWF-8HE9kf8C&oi = fnd&pg = PR3&dq = Barbero-et + al.-2012 + muscular+innervation+&ots = FCSk11AV\\_L&sig = 1LRltWiS36xz46zjTvcC-tkv2XM&redir\\_esc = y#v = onepage&q = Barbero et al.%2C 2012 muscular innervation&f = false](https://books.google.it/books?hl = it&lr = &id = rWF-8HE9kf8C&oi = fnd&pg = PR3&dq = Barbero-et + al.-2012 + muscular+innervation+&ots = FCSk11AV_L&sig = 1LRltWiS36xz46zjTvcC-tkv2XM&redir_esc = y#v = onepage&q = Barbero et al.%2C 2012 muscular innervation&f = false)
34. Ranaldi S, De Marchis C, Conforto S. An automatic, adaptive, information-based algorithm for the extraction of the sEMG envelope. *J Electromyogr Kinesiol* [Internet]. Elsevier; 2018 [cited 2019 Jul 11];42:1–9. Available from: <https://www.sciencedirect.com/science/article/pii/S1050641118301445?via%3Dihub>
35. Serrao M, Rinaldi M, Ranavolo A, Lacquaniti F, Martino G, Leonardi L, et al. Gait Patterns in patients with hereditary spastic paraparesis. Macaluso A, editor. *PLoS One* [Internet]. Public Library of Science; 2016 [cited 2019 Jul 11];11:e0164623. Available from: <https://doi.org/10.1371/journal.pone.0164623>
36. Le P, Best TM, Khan SN, Mendel E, Marras WS. A review of methods to assess coactivation in the spine. *J Electromyogr Kinesiol* [Internet]. Elsevier; 2017 [cited 2019 Jul 11];32:51–60. Available from: <https://www.sciencedirect.com/science/article/pii/S1050641116300943>
37. Rinaldi M, Ranavolo A, Conforto S, Martino G, Draicchio F, Conte C, et al. Increased lower limb muscle coactivation reduces gait performance and increases metabolic cost in patients with hereditary spastic paraparesis. *Clin Biomech* [Internet]. Elsevier; 2017 [cited 2019 Jul 11];48:63–72. Available from: <https://www.sciencedirect.com/science/article/pii/S0268003317301663>
38. Rinaldi M, D’Anna C, Schmid M, Conforto S. Assessing the influence of SNR and pre-processing filter bandwidth on the extraction of different muscle co-activation indexes from surface EMG data. *J Electromyogr Kinesiol* [Internet]. Elsevier; 2018 [cited 2019 Jul 23];43:184–92. Available from: <https://www.sciencedirect.com/science/article/pii/S1050641118302384>
39. Fisher NI. Statistical analysis of circular data [Internet]. Cambridge University Press; 1995 [cited 2019 Jul 11]. Available from: [https://books.google.it/books?hl = it&lr = &id = wGPj3EoFdlwC&oi = fnd&pg = PA1&ots = Pk0pEwyDTa&sig = snP8a\\_Q1kRZ4Z-QAJnSLvuOsnYg&redir\\_esc = y#v = onepage&q&f = false](https://books.google.it/books?hl = it&lr = &id = wGPj3EoFdlwC&oi = fnd&pg = PA1&ots = Pk0pEwyDTa&sig = snP8a_Q1kRZ4Z-QAJnSLvuOsnYg&redir_esc = y#v = onepage&q&f = false)
40. Kadaba MP, Ramakrishnan HK, Wootten ME, Gajney J, Gorton G, Cochran GVB. Repeatability of kinematic, kinetic, and electromyographic data in normal adult gait. *J Orthop Res* [Internet]. John Wiley & Sons, Ltd; 1989 [cited 2019 Jul 25];7:849–60. Available from: <https://doi.org/10.1002/jor.1100070611>
41. Steinwender G, Saraph V, Scheiber S, Zwick EB, Uitz C, Hackl K. Intrasubject repeatability of gait analysis data in normal and spastic children. *Clin Biomech* [Internet]. Elsevier; 2000 [cited 2019 Jul 11];15:134–9. Available from: <https://www.sciencedirect.com/science/article/pii/S0268003399000571>
42. Ranavolo A, Don R, Draicchio F, Bartolo M, Serrao M, Padua L, et al. Modelling the spine as a deformable body: Feasibility of reconstruction using an optoelectronic system. *Appl Ergon*

- [Internet]. Elsevier; 2013 [cited 2019 Jul 11];44:192–9. Available from: <https://www.sciencedirect.com/science/article/pii/S0003687012001111>
43. Wren TAL, Patrick Do K, Rethlefsen SA, Healy B. Cross-correlation as a method for comparing dynamic electromyography signals during gait. *J Biomech* [Internet]. Elsevier; 2006 [cited 2019 Jul 14];39:2714–8. Available from: <https://www.sciencedirect.com/science/article/pii/S0021929005004124>
  44. Nelson-Wong E, Howarth S, Winter DA, Callaghan JP. Application of autocorrelation and cross-correlation analyses in human movement and rehabilitation research. *J Orthop Sport Phys Ther* [Internet]. JOSPT, Inc. JOSPT, 1033 North Fairfax Street, Suite 304, Alexandria, VA 22134-1540; 2009 [cited 2019 Jul 11];39:287–95. Available from: <https://doi.org/10.2519/jospt.2009.2969>
  45. Cavagna GA, Kaneko M. Mechanical work and efficiency in level walking and running. *J Physiol* [Internet]. John Wiley & Sons, Ltd (10.1111); 1977 [cited 2019 Jul 11];268:467–81. Available from: <https://doi.org/10.1113/jphysiol.1977.sp011866>
  46. Don R, Ranavolo A, Cacchio A, Serrao M, Costabile F, Iachelli M, et al. Relationship between recovery of calf-muscle biomechanical properties and gait pattern following surgery for achilles tendon rupture. *Clin Biomech* [Internet]. Elsevier; 2007 [cited 2019 Jul 11];22:211–20. Available from: <https://www.sciencedirect.com/science/article/pii/S0268003306001902>
  47. Whittle MW. Three-dimensional motion of the center of gravity of the body during walking. *Hum Mov Sci* [Internet]. North-Holland; 1997 [cited 2019 Jul 11];16:347–55. Available from: <https://www.sciencedirect.com/science/article/abs/pii/S0167945796000528>
  48. Ranavolo A, Conte C, Iavicoli S, Serrao M, Silvetti A, Sandrini G, et al. Walking strategies of visually impaired people on trapezoidal-and sinusoidal-section tactile groundsurface indicators. *Ergonomics* [Internet]. Taylor & Francis; 2011 [cited 2019 Jul 11];54:246–56. Available from: <https://doi.org/10.1080/00140139.2010.548533>
  49. Cavagna GA. Within-step energy transduction [Internet]. 2002. Available from: <https://jeb.biologists.org/content/jexbio/205/21/3413.full.pdf>
  50. Faul F, Erdfelder E, Lang A-G, Buchner A. G\*Power 3: A flexible statistical power analysis program for the social, behavioral, and biomedical sciences. *Behav Res Methods* [Internet]. Springer-Verlag; 2007 [cited 2019 Jul 11];39:175–91. Available from: <https://doi.org/10.3758/BF03193146>
  51. Watson GS, Williams EJ. On the construction of significance tests on the circle and the sphere. *Biometrika* [Internet]. Oxford University Press/Biometrika Trust; 1956 [cited 2019 Jul 12];43:344. Available from: <https://www.jstor.org/stable/2332913?origin=crossref>
  52. Perry J, k S, Davids JR. Gait Analysis. *J Pediatr Orthop* [Internet]. 1992 [cited 2019 Jul 12];12:815. Available from: <https://insights.ovid.com/crossref?an=01241398-199211000-00023>
  53. Marigold DS, Patla AE. Strategies for dynamic stability during locomotion on a slippery surface: effects of prior experience and knowledge. *J Neurophysiol* [Internet]. American Physiological Society/Bethesda, MD; 2002 [cited 2019 Jul 12];88:339–53. Available from: <https://doi.org/10.1152/jn.00691.2001>
  54. Bierbaum S, Peper A, Karamanidis K, Arampatzis A. Adaptive feedback potential in dynamic stability during disturbed walking in the elderly. *J Biomech* [Internet]. Elsevier; 2011 [cited 2019 Jul 12];44:1921–6. Available from: <https://www.sciencedirect.com/science/article/abs/pii/S0021929011003472?via%3Dihub>
  55. Burden A. How should we normalize electromyograms obtained from healthy participants? What we have learned from over 25 years of research. *J Electromyogr Kinesiol* [Internet]. Elsevier; 2010 [cited 2019 Sep 17];20:1023–35. Available from: <https://www.sciencedirect.com/science/article/abs/pii/S1050641110001008>

**Publisher's Note** Springer Nature remains neutral with regard to jurisdictional claims in published maps and institutional affiliations.